一般社団法人　電子情報通信学会
THE INSTITUTE OF ELECTRONICS,
INFORMATION AND COMMUNICATION ENGINEERS

信学技報
IEICE Technical Report
A・P2022-69(2022-08)

Propagation effects of temperature variations of Moon regolith

Derek GRAY,　Konstantinos KONTIS and Julien Le KERNEC

James Watt School of Engineering,　University of Glasgow,　Glasgow,　UK
E-mail:　(Derek.Gray,　Kostas.Kontis,　Julien.LeKernec) @glasgow.ac.uk

Abstract　The Moon's surface temperature ranges from -193°C to 107°C over which the regolith relative permittivity changes from ε_r=1.4+j0.5 to ε_r=2.7.　The effects of this variation on propagation at 2.5GHz between a pair of dipoles and a pair of patches over the Moon's surface were modelled by empirical equation and full wave simulation.　The peak and null positions for each antenna configuration did not change with temperature-dependent ε_r.　The only appreciable effect was a small decrease in the peak amplitude caused by ε_r''.

Key words　radio propagation,　Moon regolith.

1. Introduction

The objective of this work is to adapt the radar equation for use on Mars.　This first paper,　however,　focuses on the Lunar surface as it is a simpler extraterrestrial case to study due to the Moon being airless with a thin diurnal dependent plasma sheath and does not have an active atmosphere with rapid gas pressure changes,　biological processes affected surfaces nor blowing dust which will affect radio propagation on Mars,　for example.　A further advantage to working on the Lunar surface first is that in situ measured topology data is available.　As a generalization,　the Lunar surface is undulating with complexity increasing with decreasing scale.

The empirical radar equation is a variation on the 2-ray interference model,　Figure 1.　There are a number of reasonable quality publications describing field trials where measured in an environment where there was only one flat reflecting surface.　The 2011 Austrian road trials at 5.6 GHz using 2 cars driving on straight sections of a highway are of interest here as the 2-ray interference pattern was evident,　as were the effects of the road roughness [1, 2].　These were used previously to introduce basic propagation concepts to MSc students in [3] instead of using a standard text like [4].　Note that in [1, 2],　it was assumed that the relative permittivity (ε_r) of the road surface was purely real.　The consequences of road surface roughness were measured but no attempt was made to modify the 2-ray interference model to account for it nor were the radiation patterns of the monopoles installed on the car rooves accounted for.

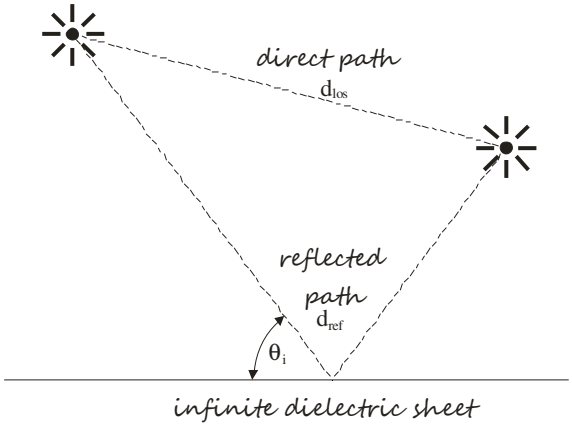

Figure 1:　Two ray interference model.

The results of a wide-ranging Lunar propagation study were detailed in [5].　The heights above the surface considered were 2,　6 and 10 m,　which were expected to be used by astronauts,　for vehicle-installed antennas and for base stations.　As a subset:　2 m to 2 m for astronaut to astronaut and 6 m to 2 m for base station to

astronaut/vehicle were considered here. As a shorthand, these cases were referred to as "2-2" and "6-2" below, respectively. Recent electrophysical consideration of Lunar regolith gave characteristics for the changes in density and ε_r within the top 1 m of the surface across the 300°C diurnal temperature range [6]. The temperature dependency of surface ε_r was summarized in Table 1. Above 0°C, the regolith appears to be a common plastic such as polyethylene or polystyrene, while below 0°C, it is a lower ε_r lossy material. Here we update [5] for 2.5 GHz in light of [6].

TABLE 1: Moon surface regolith ε_r at 1GHz, from [2].

Temperature (°C)	ε_r'	ε_r''
-193	1.4	0.08
-123	1.4	0.48
-43	1.4	0.15
27	2.5	0
107	2.7	0

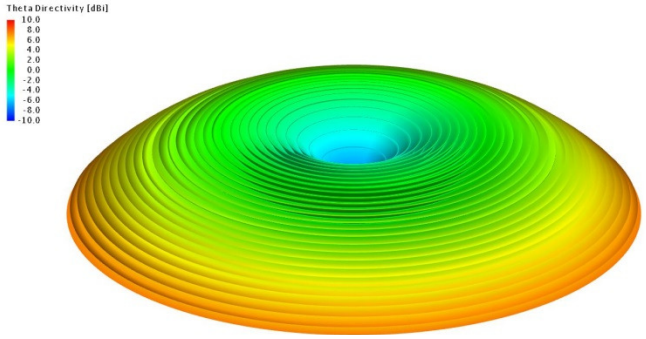

Figure 2: 3D radiation pattern of 2.5 GHz dipole 2m above infinite sheet of Moon regolith for -123°C.

Following [5], a 55.9 mm long 2 mm wide vertical dipole was simulated in FEKO™ above an infinite dielectric ground plane for each of the ε_r in Table 1, Figure 2. It is acknowledged that the ε_r'' component will likely have increased at 2.5 GHz, but no such data was available at the time of writing and we were satisfied with relative indicative computational results. As in [5], the infinite dielectric ground plane introduced ripple into the far field radiation pattern, Figures 2 to 4. For the range of angles likely to be utilized in the field across the 80° to 90° zenith range (elevation 0° to 10°), the reflected path is at or near grazing angle, and there is no effect from apparently large changes to ε_r. Between 0° to 80° zenith there were some temperature-dependent effects, but these were of the order of 1 dB, making those more or less insignificant where high elevations were used.

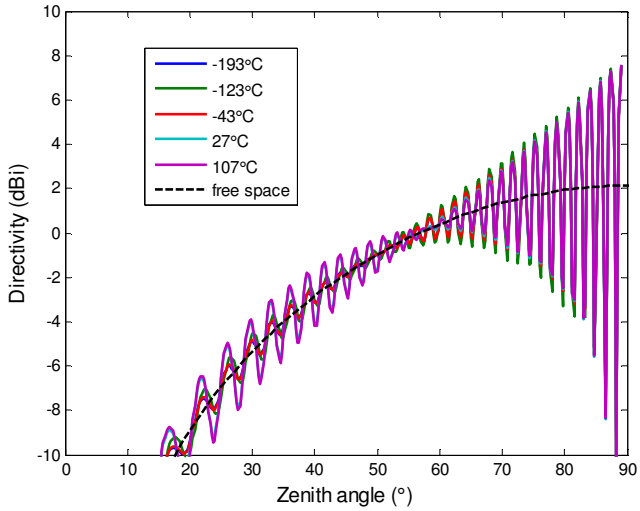

Figure 3: Effect of temperature on the zenith radiation pattern of 2.5GHz dipole 2m above an infinite sheet of Moon regolith.

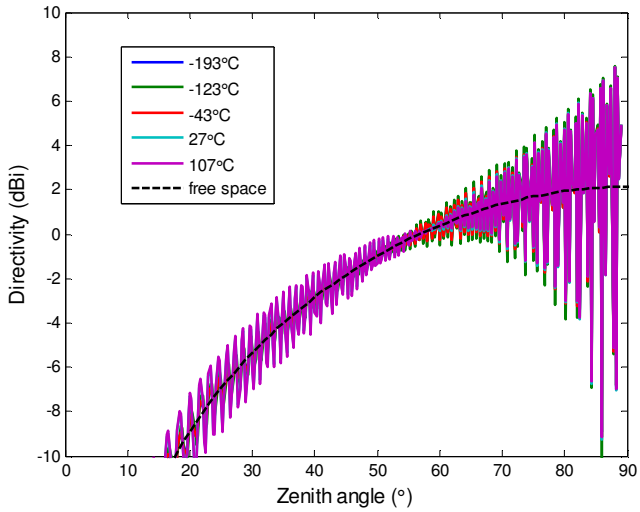

Figure 4: Effect of temperature on the zenith radiation pattern of 2.5GHz dipole 6m above an infinite sheet of Moon regolith.

Across the 80° to 90° zenith range for both heights of 2 m and 6 m, irrespective of temperature, the ripple in the dipole radiation pattern varied by 18 dB. Such a variation would affect a communications system.

2. Temperature effect on the reflection coefficient

Most texts consulted only present worked example calculations of the reflection coefficient for purely real ε_r. Interestingly [7] gives a single incident angle calculation for concrete from ITU-R P.1238, been $\varepsilon_r=7-j0.85$ which differs from the value of $\varepsilon_r=4.4$ taken from [8, 9] which was

used in [3]. The imaginary component ε_r'' introduces an additional phase shift at the point of reflection, and indicates absorption in the media [7]; the real part ε_r' indicates the degree of propagation into the reflecting surface media and the quantity of reflection. The equations from [10] were used to calculate the Normal and Parallel incidence reflection coefficients for incident elevation angles θ_i across 0° to 90°, Figures 5 to 8.

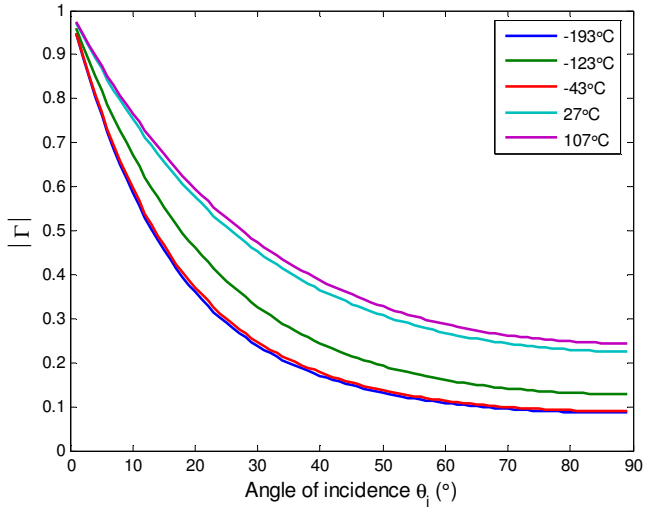

Figure 5: Lunar regolith normal incidence reflection coefficient magnitude variation with temperature (V-V case).

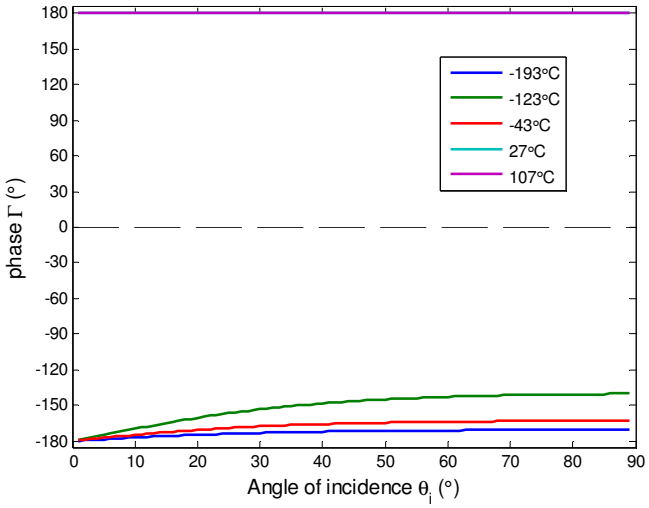

Figure 6: Lunar regolith normal incidence reflection coefficient phase variation with temperature (V-V case).

For both V-V and H-H the purely real 27 and 107°C reflection coefficients were very close in both magnitude and phase, Figures 5 to 8. Similarly, -193 and -43°C also formed a pair having very close magnitude and phase. The reflection coefficients for -123°C magnitude and phase lay between the 2 pairs. There were significant variation in magnitude and phase across the 300°C range, indicating that the different ε_r must be taken into account in designing any Lunar communications link.

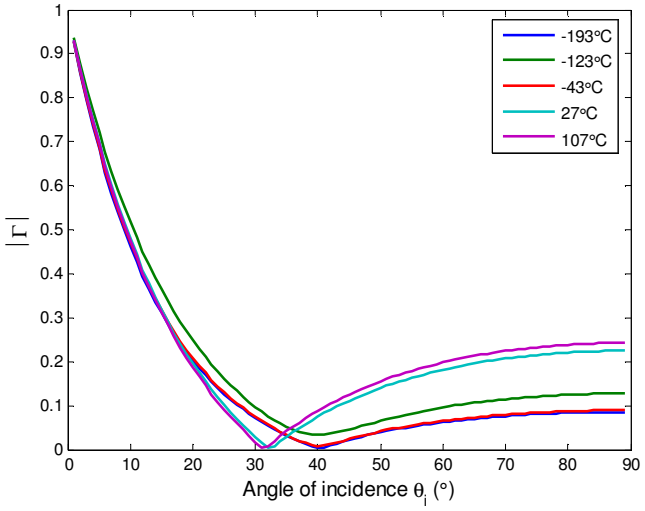

Figure 7: Lunar regolith parallel incidence reflection coefficient magnitude variation with temperature (H-H case).

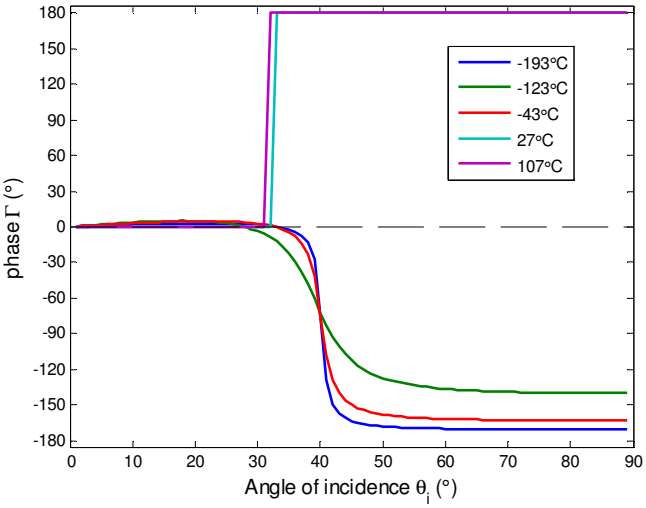

Figure 8: Lunar regolith parallel incidence reflection coefficient phase variation with temperature (H-H case).

3. Propagation over concrete

Given the lack of accessibility to the Lunar surface, benchmarking of the FEKO™ models was done against existing measured data from a flat dry concrete floor described in [3]. The measurements were made along a 40 m diagonal transect in an event space hall that was 35.4 x 28.6 m with a 6 m ceiling, Figure 9. The air-suspended square patch had a side length of 54 mm, was 5 mm above a 300 x 300 mm aluminium ground plane,

and gave 9.4 dBi at 2.5 GHz, Figure 10. These antennas were more or less equivalent to the cantennas described in [3] and thus are interchangeable.

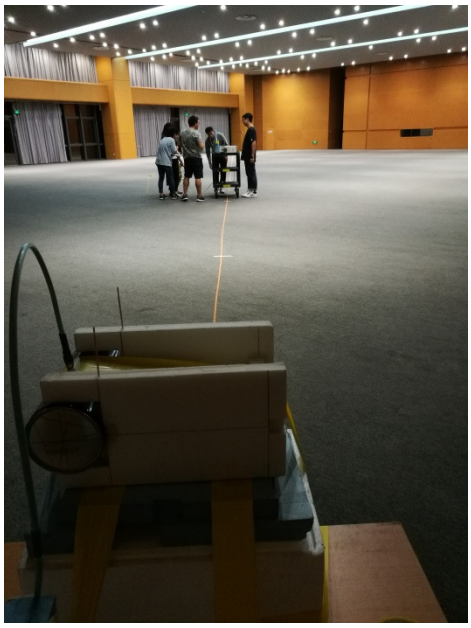

Figure 9: Photograph of Tx antenna and Rx trolley during measurements in a hall with the transect marked by yellow tape, from [3].

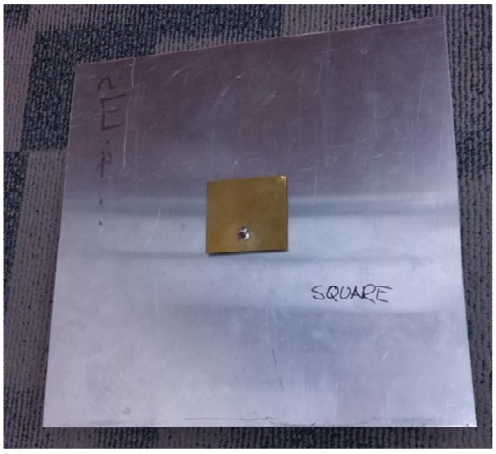

Figure 10: Photograph of 2.5GHz patch antenna.

The breakpoint is a useful landmark for simple propagation studies [7]. At distances less than the breakpoint, the signal strength oscillates due to constructive and destructive interference, with the peaks following the trend of the free space loss [7]. Beyond the breakpoint, the signal reduces with a smooth trend closer to 40log(distance) due to destructive interference as the difference between the direct and the reflected paths trend toward cancelation. For 2.5 GHz, the breakpoint for 1-1 is 33.4 m, 2-2 is 133.4 m and 400.3 m for 6-2. Thus measuring to 40 m diagonally across the event space hall for 1-1 included the breakpoint and thus all of the peaks and nulls. Note that the peaks and nulls of the oscillations in the vertically (V-V) and horizontally (H-H) polarized cases did not align due to the polarization-derived differences in the reflection coefficient, Figures 11 and 12 [3]. The FEKO™ patch-to-patch model agreed favorably with the prior cantenna work, confirming the soundness of the simulation model. The concrete floor was represented as an infinite dielectric ground plane with ε_r=4.4 from [8, 9] in the theoretical 2-ray calculations and the FEKO™ models.

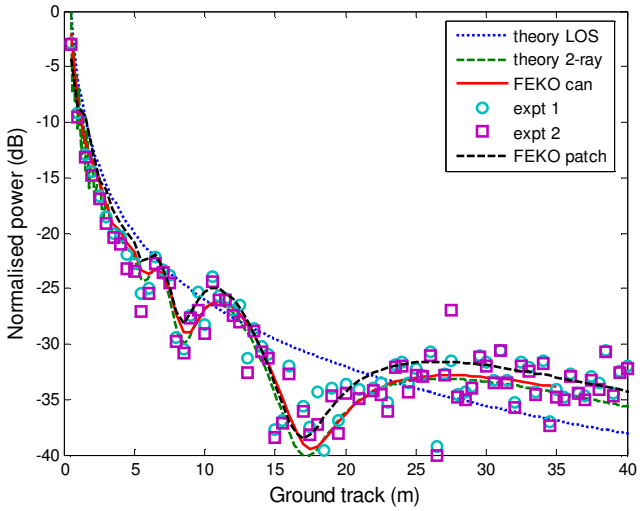

Figure 11: Theoretical, simulated, and measured Rx power over concrete 1m above floor, vertically polarized.

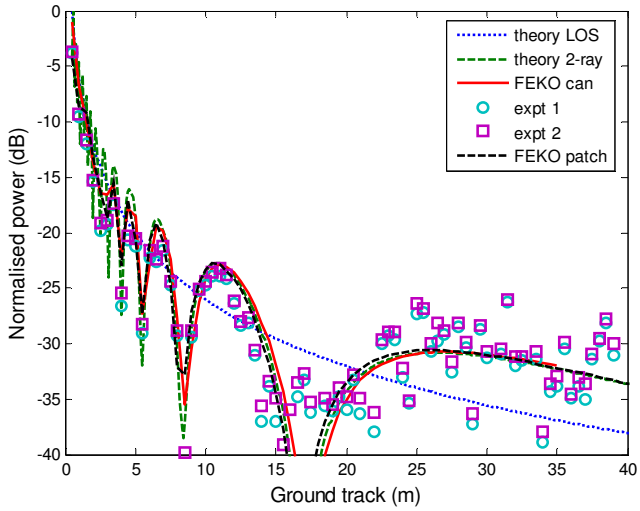

Figure 12: Theoretical, simulated, and measured Rx power over concrete 1m above floor, horizontally polarized.

As a further check, the FEKO™ patch-to-patch model was rerun for increasing heights above the concrete floor,

Figure 13. Increasing the antenna height caused the series of peaks and nulls to stretch out to greater distances, conforming with increased breakpoint value. The positions of the peaks and nulls for both polarizations at a given height always aligned, but the H-H case had slightly higher peaks and deeper nulls.

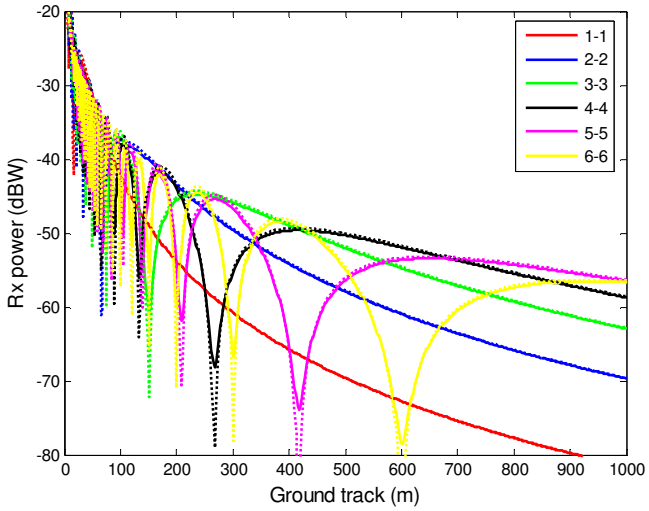

Figure 13: Equal patch height cases over concrete; heights in metres; '–' was V-V, '····' was H-H, from FEKO™.

4. Propagation over Moon regolith

Having created patch-to-patch and dipole-to-dipole models in FEKO™, all 5 temperatures were run for the 2-2 and 6-2 cases to model astronaut-to-astronaut and base station-to-astronaut communications. The 2-2 results are presented with axis aligned antennas in free space, while the 6-2 results are compared to antennas in free space with a 4m vertical offset, Figures 14 to 17. For brevity, only the extreme cases -193°C and 107°C are shown.

As a generalization, a given antenna pair in a given configuration gave almost identical results irrespective of temperature, in stark contrast to what was expected from examining the temperature effects on the reflection coefficient above. Comparing the V-V to H-H, the H-H always gave slightly higher peaks and slightly deeper nulls than the V-V, as was observed with the 1-1 to 6-6 concrete simulations.

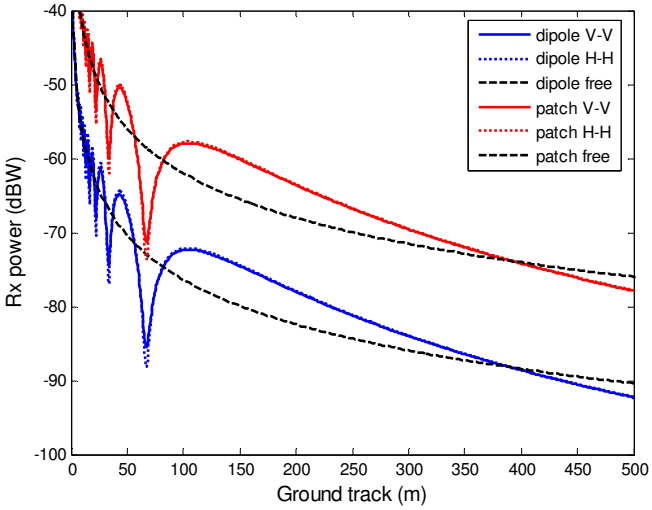

Figure 14: Coupling of dipole and patch pairs over regolith for 2-2 case at -193°C; from FEKO™.

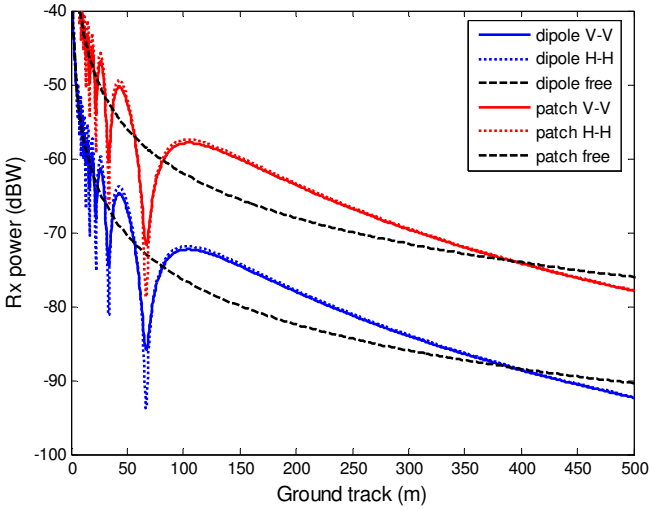

Figure 15: Coupling of dipole and patch pairs over regolith for 2-2 case at 107°C; from FEKO™.

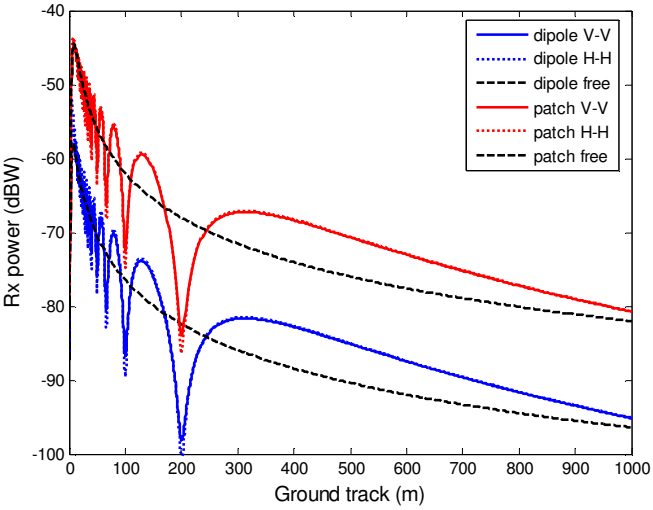

Figure 16: Coupling of dipole and patch pairs over regolith for 6-2 case at -193°C; from FEKO™.

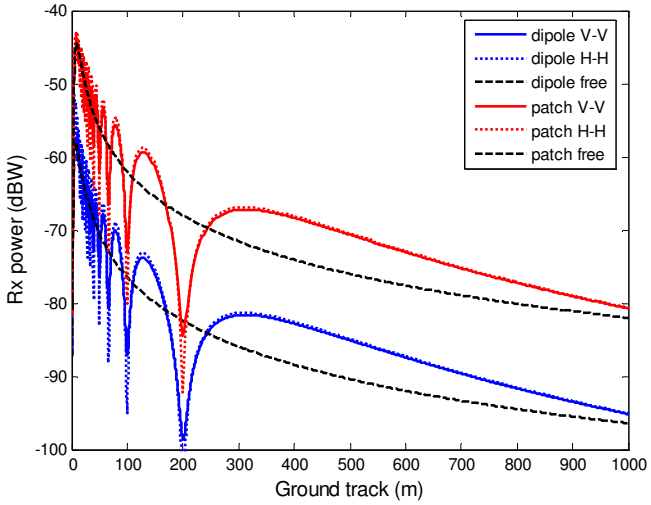

Figure 17: Coupling of dipole and patch pairs over regolith for 6-2 case at 107°C; from FEKO™.

Given the small differences between the different temperatures and configurations, it was necessary to take one dataset as a reference and subtract the other datasets for each comparison. Thus the following observations were made:

Excluding the changes in null depth, the temperature changes across -193 to 107°C caused less than 0.6 dB variation in signal strength for H polarization, and less than 0.4 dB for the V polarization.

The V and H polarization differences for dipoles and patches were near identical: H polarized always had higher peaks and lower nulls than V polarized, thus H had the greater signal strength range of either polarization.

For the 6-2 cases, the V/H difference was least at 0.5dB at 79 m for -43 and -193°C, whereas greatest difference was 1.1 dB for 27 and 107°C. Likewise the V/H difference range envelope was 3.5dB for -43 and -193°C and 9.3 dB for 27 and 107°C. So, an astronaut walking away from a base station during the night could expect about 6dB less signal strength variation than they would experience during the day. As with the V to H polarization comparison, the signal strength variations found in the FEKO™ simulation results were not significant.

7. Conclusions and future work

The effects of the changes in ε_r of Lunar regolith on 2 simple propagation cases over infinite flat ground planes were simulated in a commercially available MoM software. All dipole and microstrip antenna cases trialed gave results that conformed with expected 2-ray interference patterns. The maximum difference found for both the ε_r variation across 300°C temperature and changing polarization was 1.1 dB. This was considered to be an insignificant Rx power variation and would be difficult to measure in the field. Of much greater concern is the 18 dB directivity (and thus power) range seen across 0° to 5° elevation range in the radiation pattern of a vertical dipole over an infinite dielectric sheet.

Future work will consider the effects of regolith surface roughness by incorporating measured Lunar surface topology. It is expected these effects will be significant as road roughness is in terrestrial road trials.

8. References

[1] C. Sommer & F. Dressler, "Using the right two-ray model? a measurement-based evaluation of PHY models in VANETs," *Int. Conf. on Mobile Computing and Networking (MobiCom 2011)*, Las Vegas, NV, Sept. 2011.

[2] C. Sommer, S. Joerer & F. Dressler, "On the applicability of two-ray path loss models for vehicular network simulation," *IEEE Vehicular Networking Conference (VNC)*, 2012.

[3] D. Gray, J. Wang & M. Leach, "Propagation exercise for mixed Masters level introductory mobile communications course," *IEICE Tech. Rep.*, Kikaishinko-kaikan, Tokyo, vol. 121, no. 305, AP2021-129, December 2021.

[4] T.S. Rappaport, *Wireless communications: principals and practice*, 1st ed., Prentice Hall, 1995.

[5] S.U. Hwu, M. Upanavage & C. Sham, "Lunar surface propagation modeling and effects on communications," *26th International Communications Satellite Systems Conference (ICSSC)*, Jan. 1, 2008.

[6] V. Yushkov, I. Kibardina & O. Yushkova, "Modeling of electrophysical properties of the Moon ground," *Russian Open Conference on Radio Wave Propagation (RWP)*, 2019.

[7] C. Haslett, *Essentials of radio propagation*, Cambridge, 2008.

[8] H.C. Rhim & O. Buyukozturk, "Electromagnetic properties of concrete at microwave frequency range," *ACI Materials Journal*, title no. 95-M25, 1998.

[9] O. Buyukozturk, T.-Y. Yu & J.A. Ortega, "A methodology for determining complex permittivity of construction materials based on transmission-only coherent, wide-bandwidth free-space measurements," *Cement & Concrete Composites*, pp. 349–359, 2006.

[10] F. Ulaby, E. Michielssen & U. Ravaioli, *Fundamentals of applied electromagnetics*, 6th ed. Upper Saddle River, NJ: Pearson, 2010.